

## Kinetic and Structural Characterization of Slr0077/SufS, the Essential Cysteine Desulfurase from *Synechocystis* sp. PCC 6803<sup>†,‡</sup>

Bhramara Tirupati,<sup>‡</sup> Jessica Lynn Vey,<sup>||</sup> Catherine L. Drennan,<sup>||</sup> and J. Martin Bollinger, Jr.\*<sup>‡,§</sup>

Department of Biochemistry and Molecular Biology and Department of Chemistry, The Pennsylvania State University, University Park, Pennsylvania 16802, and Department of Chemistry, Massachusetts Institute of Technology, Cambridge, Massachusetts 02139

Received April 28, 2004; Revised Manuscript Received July 12, 2004

**ABSTRACT:** Cysteine desulfurases, designated NifS, IscS, and SufS, cleave L-cysteine to form alanine and an enzyme cysteinyl persulfide intermediate. Genetic studies on the photosynthetic cyanobacterium *Synechocystis* sp. PCC 6803 have shown that of the three Nif/Isc/SufS-like proteins encoded in its genome only the sequence group II protein, Slr0077/SufS, is essential. This protein has been overexpressed in *Escherichia coli*, purified to homogeneity, shown to bind pyridoxal-5'-phosphate (PLP) and to catalyze cysteine desulfuration, and characterized in terms of its structure and kinetics. The results suggest that catalysis in the absence of accessory factors has two constituent pathways, one involving nucleophilic attack by C372 to form the Slr0077/SufS-bound cysteinyl persulfide intermediate and the second involving intermolecular attack by the sulfur of a second molecule of the substrate on the initial L-cysteine–PLP complex to form free L-cysteine persulfide. The second pathway is operant in the C372A variant protein, explaining why it retains significant activity, which is proportional to the concentration of L-cysteine (i.e., does not saturate). C–S bond cleavage by the first (normal) pathway is considerably less efficient than the equivalent step in a group I desulfurase (Slr0387) from the same organism (characterized in the accompanying paper). The 1.8 Å crystal structure of the protein, which is very similar to that previously reported for *E. coli* SufS, shows that the loop on which C372 resides is well-ordered and shorter by 11 residues than the corresponding disordered loop of the group I NifS-like protein from *Thermotoga maritima*. Sequence comparisons establish that the *T. maritima* and Slr0387 proteins have loops of similar length. The combined structural and kinetic data imply that the modest activity of Slr0077/SufS and other SufS proteins in comparison to their sequence group I (NifS/IscS-like) paralogues results from inefficiency in the nucleophilic attack step associated with differences in the structure or dynamics of this loop. The recent reports that SufS proteins can be activated manyfold by binding to SufE thus implies that the accessory protein either accelerates nucleophilic attack by the conserved cysteine residue of SufS by a conformational mechanism or itself contributes a nucleophilic cysteine for more efficient intermolecular attack.

Cysteine desulfurases (CDs)<sup>1</sup> mobilize sulfur for incorporation into iron–sulfur clusters (1–10), thiamin (11, 12), molybdopterin (13), and the modified tRNA base thiouridine (14–16). Proven or apparent homologues of the first CD to be discovered, the NifS protein from *Azotobacter vinelandii* (2), have been identified in organisms from all three domains of life. The NifS-like proteins have been divided on the basis

of sequence similarity relationships into groups I and II (17), and genes encoding them have been found in at least three distinct genetic contexts (1, 5, 18, 19). The NifS proteins themselves, which belong to sequence group I (17), are encoded in clusters of genes that include those for the nitrogenase component proteins and other accessory factors involved in the posttranslational processing of the nitrogenase components (1, 18). The CD and the additional accessory factors cooperate to assemble and insert the multiple catalytically essential FeS clusters into the nitrogenase components (1, 3). Inactivation of the *nifS* gene in *A. vinelandii* compromises diazotrophy but does not otherwise impair the bacterium (1). A second subset of group I NifS-like proteins, found both in diazotrophic species such as *A. vinelandii* and in nondiazotrophic species from the Bacteria and Eukarya domains, are encoded in gene clusters that have been designated *isc* (for iron sulfur cluster synthesis) (4, 5). The *isc* gene clusters also encode additional proteins with proven or proposed roles in FeS cluster assembly and insertion (5). Genetic experiments have generally revealed important or essential functions for CDs encoded in *isc* clusters (IscS

<sup>†</sup> This research was supported by NSF (Grant MCB-0235979 to J.M.B.), NIH (Grant GM69857 to C.L.D.), The William Asbjornsen Albert Memorial Fellowship (to J.L.V.), and the Corning Foundation Fellowship (to J.L.V.). The data collection facilities at the Advanced Light Source are funded by the U.S. Department of Energy, Office of Basic Research.

<sup>‡</sup> Coordinates of the structure have been deposited in the Protein Data Bank ([www.rcsb.org/pdb/](http://www.rcsb.org/pdb/)) with accession code 1T3I.

\* Address correspondence to this author. Tel: (814) 863-5707. Fax: (814) 863-7024. E-mail: [jmb21@psu.edu](mailto:jmb21@psu.edu).

<sup>||</sup> Department of Biochemistry and Molecular Biology, The Pennsylvania State University.

<sup>§</sup> Department of Chemistry, The Pennsylvania State University.

<sup>||</sup> Department of Chemistry, Massachusetts Institute of Technology.

<sup>1</sup> Abbreviations: PLP, pyridoxal-5'-phosphate; DTT, dithiothreitol; CD, cysteine desulfurase; FeS, iron–sulfur.

proteins). In *A. vinelandii*, *Helicobacter pylori*, and *Saccharomyces cerevisiae*, the *iscS* gene was found to be rigorously essential, whereas disruption of the *Escherichia coli* *iscS* gene was not lethal but resulted in multiple auxotrophies and biochemical deficiencies (5, 6, 20, 21).

A third less extensively characterized genetic context in which genes for NifS-like proteins are found has been designated *suf*, for sulfur utilization (19, 22, 23). These NifS-like proteins (SufS) invariably belong to sequence group II (17). Several recent observations have established links between proteins encoded in *suf* operons and FeS assembly. First, the *suf* operons in several organisms (e.g., *E. coli* and *Erwinia chrysanthemi*) encode homologues of the protein IscA (SufA) (19, 24). IscA is thought to serve as a scaffold for assembly of FeS clusters by the Isc system (8). Second, recent analyses have shown that transcription of *suf* genes is activated in response to oxidative stress (a condition known to damage FeS clusters in enzymes) and iron limitation (23, 25, 26). Third and most compellingly, Takahashi and Tokumoto recently showed that the auxotrophies associated with deletion of the entire *isc* cluster in *E. coli* could be corrected by overexpression of the *suf* operon (27). They further showed that, whereas the *suf* genes are dispensable in a wild-type background, all but one of the genes (*sufD*) is rendered essential by the absence of a functional *isc* operon (27).

The above genetic experiments with *A. vinelandii* and *E. coli* provide evidence that the multiplicity of CDs in many bacterial species reflects functional specialization. For example, the data suggest that the *A. vinelandii* NifS protein functions solely in processing of nitrogenase, whereas the IscS CD is required for less-specialized metabolic functions (termed "housekeeping" by Dean and co-workers) (5). NifS may be required merely to cope with the very high demand for FeS synthesis created by the high prevalence of the nitrogenase enzyme, or it may be uniquely competent to interact with the other Nif proteins that are required for nitrogenase cluster insertion (e.g., NifU). Clearly, NifS is incompetent for some subset of the essential functions of IscS (5). Similarly, the simplest interpretation of the *E. coli* genetic studies is that IscS serves most, if not all, of the essential FeS assembly functions but is dispensable because of the presence of the SufS-associated "back-up" system (27). Importantly, the data provide argument that SufS cannot, in the absence of the other constituents of the Suf system, assume the functions of IscS, even when SufS is overexpressed (27). This observation suggests that the details of FeS cluster assembly or the nature of protein-protein interactions (or both) differ significantly in the two systems. Indeed, recent studies have demonstrated the association of SufS proteins with other Suf proteins. In the first study, association with SufE was found to increase the desulfurase activity of SufS from *Erwinia chrysanthemi* by ~40-fold (28). This group subsequently demonstrated transfer of the sulfur from the SufS persulfide to SufE and suggested that acceleration of persulfide cleavage is primarily responsible for the observed activation (29). In another study, SufS from *E. coli* was found to form a complex with SufB, -C, -D, and -E, again increasing activity by manyfold (30).

Like that of *E. coli*, the genome of the freshwater, photosynthetic cyanobacterium *Synechocystis* sp. PCC 6803 encodes three NifS-like proteins (Slr0387, Slr0704, and

Slr0077) (31, 32). Slr0387 and Slr0704 are members of sequence group I, whereas Slr0077 belongs to group II (17). Although the cyanobacterial genome lacks a recognizable *isc* gene cluster (the genes encoding the two group I CDs appear to be isolated), it does possess a *suf* cluster, albeit one with homologues of only four (*sufBCDS*) of the six genes in the *E. coli* *suf* cluster (*sufABCDSE*) (27). Studies by our group and others have established that *slr0387* and *slr0704* can be disrupted either singly or in combination without abolishing the ability of the bacterium to grow photoautotrophically in minimal medium (33).<sup>2</sup> By contrast, targeted disruption of *slr0077* has to date yielded only merodiploid strains, implying that this gene is essential (33).<sup>2</sup> Similarly a SufS homologue, *csd* (*yurw*) was found to be essential for the survival of *Bacillus subtilis* (34). To our knowledge, *Synechocystis* sp. PCC 6803 and *B. subtilis* are the only two organisms for which SufS is essential. It is likely that the situation in cyanobacteria is relevant to FeS assembly in plants (more specifically, in their photosynthetic organelle, the chloroplast). ATP- and light-dependent FeS assembly has been demonstrated in chloroplasts (35), and a gene for a group II desulfurase with a putative plastid localization sequence has recently been identified in the genome of *Arabidopsis thaliana* (36, 37). The predicted protein is 62% identical with *Synechocystis* sp. PCC 6803 Slr0077/SufS. Moreover, apparent homologues of *sufB* and -C have also been identified in the plastid genome of red algae and in the nuclear genome of *A. thaliana* (22, 38, 39), and the nucleus-encoded *A. thaliana* SufB and -C proteins have probable plastid targeting sequences. Thus, the *suf* system is clearly present in chloroplasts, and given that the sole group I CD identified in plants appears to be targeted to the mitochondria (40), SufS is likely to have a primary role in chloroplast FeS assembly, as it appears to have in cyanobacteria.

The two dispensable sequence group I CDs from *Synechocystis* sp. PCC 6803 have been overexpressed in and purified from *E. coli* (41, 42). They were demonstrated to have the expected cysteine desulfurase activity, and their steady-state kinetic behavior was partially characterized. By contrast, no purification or characterization of the essential Slr0077/SufS (hereafter, simply SufS) has been reported. In this work, we report the overexpression, purification, and structural and preliminary kinetic characterization of SufS from *Synechocystis* sp. PCC 6803. The results suggest that, in the absence of accessory factors, formation of the enzyme cysteinyl persulfide intermediate upon attack on the substrate sulfur by the C372 thiol(ate) is ~1000-fold slower than the corresponding step in a group I CD, Slr0387, from the same organism (43). If applicable to SufS proteins from other organisms, this conclusion would imply that activation of the SufS CDs by other Suf proteins (especially SufE) must involve acceleration of the persulfide formation in addition to (or instead of) the previously proposed acceleration of breakdown of the persulfide intermediate by sulfur transfer (29).

## MATERIALS AND METHODS

**Materials.** Restriction enzymes, *Nde*I, *Eco*R1, and *Bgl*II, were purchased from New England Biolabs. L-Cysteine, Tris,

<sup>2</sup> Tirupati, B., Behshad, E., Shen, G., Wang, T., Parkin, S. E., Golbeck, J. H., Bryant, D. A., and Bollinger, J. M., Jr., manuscript in preparation.

magnesium chloride, and glycerol were obtained from Sigma. Poly(ethylene glycol) 4000 (PEG 4000) was obtained from Fluka. *n*-Octanoyl sucrose was obtained from Hampton Research (Laguna, CA). [ $^{35}$ S]-L-Cysteine was purchased from PerkinElmer Life Sciences, Inc., and had a specific activity of 1075.0 Ci/mmol.

**Cloning, PCR, and Site-Directed Mutagenesis.** The open reading frame of *slr0077* was amplified from the genomic DNA of *Synechocystis* sp. PCC 6803 by using the primers *slr0077N*-Terminus (5'-CTTTGATTTTAAACATATGGT-TGCTCT-3') and *slr0077C*-Terminus (5'-CAGAATTCG-GTTTGCTGAGGCAG-3'). The PCR product generated was digested with the restriction enzymes *NdeI* and *EcoRI* and ligated into the *NdeI* and *EcoRI* sites of pET22b (Novagen) to generate the expression plasmid pET22bSlr0077. This expression plasmid was used as a PCR template to generate the coding sequence for the C372A variant protein. A fragment containing the 5'-most 1143 bp of the gene was generated by using *slr0077N*-terminal and C372ABgIIIR (5'-CGGTTGGGTGGCATGGTGGCCAGATCTGATGGC-3') primers. The 3' fragment (197 bp) was generated by using *slr0077C*-terminal and C372ABgIIIF (5'-CGCCATCA-GATCTGGGCACCATGCCACCAACCG-3') primers. By combining the two PCR products as templates and using the *slr0077* N-terminal and C-terminal primers, the fused coding sequence of the C372A variant was amplified by PCR. This PCR product was digested with *NdeI* and *EcoRI* and cloned into the *NdeI* and *EcoRI* sites of pET22b (Novagen) to generate the expression plasmid pET22bC372A. The presence of only the desired substitution in the resulting plasmid was verified by sequencing of the entire coding region. DNA sequence determinations were carried out by the Penn State Nucleic Acid Facility.

**Overexpression and Purification of SufS and SufS-C372A.** Expression of SufS and SufS-C372A was achieved by using BL21(DE3) Star cells (Invitrogen) transformed with the plasmids described above. Cells were grown at 37 °C in rich LB broth (3.5% tryptone, 2.0% yeast extract, and 0.5% sodium chloride) containing 150 mg/L ampicillin to an OD<sub>600</sub> of 0.7–0.8, induced by addition of 200  $\mu$ M IPTG, and grown for 20–24 h at 16–20 °C. The cells were then harvested by centrifugation and stored at –80 °C.

All steps in the purification were carried out at 4 °C. The frozen cells were thawed in 50 mM Tris-HCl buffer, pH 7.8, containing 0.005% phenylmethylsulfonylfluoride (PMSF) and lysed in a French pressure cell. Cell debris was removed by centrifugation at 12 000g for 10 min. To the supernatant was added 176 g/L ammonium sulfate (30% of saturation), and the suspension was centrifuged at 12 000g for 10 min. An additional 127 g/L of ammonium sulfate (50% of saturation) was added to the supernatant, and the suspension was again centrifuged as before. The pellet was dissolved in a minimum volume of 50 mM Tris-HCl, pH 7.8, and the solution was dialyzed overnight against 4 L of the same buffer. The dialyzed protein was applied to a Q-Sepharose Fast Flow column (185 mL, Pharmacia Biotech) and eluted with a 1.5 L linear gradient of 0–1 M NaCl at a flow-rate of 3 mL/min. Fractions containing SufS were pooled, and the pool was concentrated and dialyzed against 4 L of 50 mM Tris-HCl buffer, pH 7.8, containing 100  $\mu$ M PLP. The dialyzed protein was either stored in 10% glycerol for further purification at a later time or loaded onto a MonoQ HR 10/

10 column (Pharmacia) and eluted with a 220 mL linear gradient of 0–1 M NaCl at a flow-rate of 1 mL/min. Fractions containing SufS were pooled, concentrated, and dialyzed against 4 L of 100 mM Na-HEPES, pH 7.8. Final purification was achieved by chromatography on a Superose 12 HR 10/30 column (Pharmacia). The protein was eluted with 100 mM Na-HEPES, pH 7.8, at a flow-rate of 0.4 mL/min. The purity of the protein preparation was estimated by denaturing polyacrylamide gel electrophoresis with Coomassie staining to be >90%.

**Quantitation of Bound Pyridoxal-5'-phosphate.** PLP bound to SufS was quantified as described previously (44).

**Kinetics of Substrate C–S Bond Cleavage.** SufS (10  $\mu$ M) and [ $^{35}$ S]-L-cysteine (5  $\mu$ M, (4–7)  $\times$  10<sup>5</sup> cpm per assay) were incubated at 21 °C in a total reaction volume of 80  $\mu$ L. At various times, a 7.5  $\mu$ L aliquot of the reaction was added to 7.5  $\mu$ L of a solution of 2 $\times$  SDS–PAGE loading buffer (0.25 M Tris-HCl, pH 6.8, 4% SDS, 20% glycerol, and trace bromophenol blue) that had been preheated to 90 °C in a heat block. After incubation at 90 °C for 4 min, the protein was resolved on a 15% Tris-HCl polyacrylamide gel, and radiolabel on the protein was quantified by phosphorimager analysis. In another experiment, SufS (10  $\mu$ M) and [ $^{35}$ S]-L-cysteine (5  $\mu$ M, (4–7)  $\times$  10<sup>5</sup> cpm per assay) were incubated at 21 °C in a total reaction volume of 200  $\mu$ L. At various times, a 20  $\mu$ L aliquot of the reaction was mixed with 80  $\mu$ L of a reducing quench solution (125 mM DTT and either 12.5% sodium dodecyl sulfate or 5 M guanidine hydrochloride) that had been preheated to 90 °C in a heat block. After a 15 min incubation at 90 °C, 5  $\mu$ L of 0.72 N sulfuric acid was added to each sample. Incubation at room temperature for another 20 min allowed for volatilization of the hydrogen sulfide. The radioactivity remaining in each sample was quantified by liquid scintillation counting.

**Cysteine Desulfurase Assays.** The standard assay mix had [ $^{35}$ S]-L-cysteine ((4–7)  $\times$  10<sup>5</sup> cpm per assay), 100 mM Na-HEPES, pH 7.8, 50 mM dithiothreitol (DTT), and 5  $\mu$ M enzyme in a 100  $\mu$ L reaction mix. The reaction mix was held in an inverted 1.5 mL eppendorf tube cap placed at the bottom of the scintillation vial. The scintillation vial was capped with an open faced screw cap containing a silicone–Teflon septum. The septum allowed the addition of 1 mL of 0.72 N sulfuric acid with a syringe to quench the reaction and also prevented the product (hydrogen sulfide) from escaping. The hydrogen sulfide volatilized was trapped by 500  $\mu$ L of 10 mM sodium hydroxide that was prevented from mixing with the reaction solution by being held in a plastic tube that was placed inside the scintillation vial. The trapping reaction was allowed to proceed for 1 h. The volatile H<sub>2</sub>S trapped as sodium sulfide was transferred to another scintillation vial and quantified separately from the unreacted cysteine by liquid scintillation counting.

**Crystallization and Data Collection.** Standard hanging drop vapor diffusion methods were used to crystallize SufS at 4 °C over a reservoir solution of 0.1 M Tris-HCl, pH 8.0, 0.25 M MgCl<sub>2</sub>, and 25% PEG 4000. Optimal crystals were grown from drops made by mixing 2  $\mu$ L of protein stock solution (17 mg/mL SufS in 100 mM HEPES, pH 7.8, with 3% glycerol), 0.5  $\mu$ L of adjusted well solution (0.1 M Tris, pH 8.0, 0.3 M MgCl<sub>2</sub>, 28% PEG 4000), 0.2  $\mu$ L of micro-seeding solution (1:10 000 dilution of crystals grown over the above reservoir solution), and 0.3  $\mu$ L of *n*-octanoyl



Table 1: Data Collection Statistics

wavelength (Å)	1.100
resolution (Å)	50–1.80
$R_{\text{sym}}$ (%) <sup>a,b</sup>	6.2 (32.4)
total observations	979 036
unique reflections	99 625
avg redundancy	4
$\langle I/\sigma \rangle$ <sup>b</sup>	18.1 (4.5)
completeness (%) <sup>b</sup>	94.4 (82.2)

<sup>a</sup>  $R_{\text{sym}} = (\sum_{hkl} \sum_i |I_i(hkl) - \langle I(hkl) \rangle|) / (\sum_{hkl} \sum_i I_i(hkl))$  for  $n$  independent reflections and  $i$  observations of a given reflection.  $\langle I(hkl) \rangle =$  average intensity of the  $i$ th observation. <sup>b</sup> Numbers for the highest resolution shell are shown in parentheses.

Table 2: Refinement Statistics

resolution (Å)	50–1.80
reflections (working/test)	85 453/9531
$R_{\text{cryst}}/R_{\text{free}}$ (%) <sup>a</sup>	19.4/21.8
residues	811
total protein atoms	6213
total ligand atoms	81
total solvent atoms	538
disordered side chains <sup>b</sup>	13/9
rms deviation	
bonds (Å)	0.0098
angles (deg)	1.35
Ramachandran analysis	
most-favored	655 (91.1%)
allowed	60 (8.6%)
generously allowed	2 (0.3%)
disallowed	0

<sup>a</sup>  $R_{\text{cryst}} = \sum_h ||F_o(h)| - |F_c(h)|| / \sum_h |F_o(h)|$ , where  $F_o$  and  $F_c$  are the observed and calculated structure factors, respectively.  $R_{\text{free}}$  is calculated using the same equation with a test set of reflections that are not used during refinement. <sup>b</sup> Chain A/chain B.

sucrose detergent. Crystals grown from these conditions appeared in 1–2 days, and all had an intense yellow color, presumably due to bound PLP. Prior to data collection, crystals were transferred to reservoir solution with 20% glycerol for 30 s and flash-cooled in liquid nitrogen. The crystals belong to the space group  $P2_12_12_1$  with unit cell dimensions  $a = 88.9$ ,  $b = 89.3$ , and  $c = 142.0$  Å and contain two molecules of SufS per asymmetric unit. Data were collected to 1.8 Å resolution at ALS beamline 5.0.2 and reduced using DENZO and SCALEPACK (45). Table 1 summarizes the data collection statistics.

**Structure Determination and Refinement.** The structure of SufS was determined by molecular replacement with AmoRe (46) using a polyalanine-substituted model derived from *E. coli* SufS (1JF9.pdb) (47). Refinement was carried out with CNS (48), protein model building was done in XtalView (49, 50), and construction and fitting of *n*-octanoyl sucrose were accomplished with Quanta (Molecular Simulations, Inc). Composite simulated annealing omit electron density maps calculated in CNS were used to check this model (45). Of 420 residues per monomer, residues 7–414 were observed in electron density maps with one chain break per molecule (from 60 to 61 in chain A, and from 60 to 62 in chain B). Table 2 summarizes refinement statistics.

## RESULTS AND DISCUSSION

**Expression and Purification of SufS.** Problems encountered in overexpression of SufS (see Supporting Information) were overcome by using a ribonuclease E-deficient strain of *E. coli* (BL21(DE3) Star cells from Invitrogen) as expression

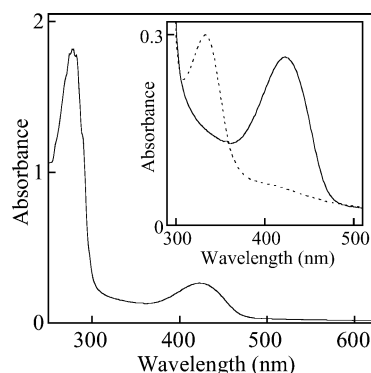


FIGURE 1: Absorption spectrum of SufS and change upon reduction with sodium borohydride (NaBH<sub>4</sub>). The main panel shows the full spectrum of the native protein. The inset shows the region of the spectrum corresponding to absorption from PLP (solid trace) and the spectrum resulting from reduction of the protein with NaBH<sub>4</sub> (dotted trace). The SufS concentration was 100 μM.

host. Accumulation of a protein with the correct apparent molecular weight of ~47 kDa was observed in extracts of this strain (see Supporting Information, Figure S1). Purification of SufS from these cells as described in Materials and Methods typically yielded 2–4 mg of protein per gram of wet cell mass. Because this yield is lower than has been observed in expression of other *Synechocystis* sp. PCC 6803 proteins in *E. coli*, the N-terminal sequence of the purified protein was determined to verify that SufS had, in fact, been isolated. The first five residues were as predicted by the translated *slr0077* gene sequence under the assumption of posttranslational removal of the initiator methionine residue.

**PLP Content of Pure Recombinant SufS.** Pure SufS exhibits the bright yellow color characteristic of PLP-containing enzymes and absorption maxima for the protein at 278 nm and for the cofactor at 425 nm (Figure 1). The  $\lambda_{\text{max}}$  of the cofactor suggests that it is fully protonated at this pH (7.8). Addition of sodium borohydride to the enzyme changes its absorption spectrum to  $\lambda_{\text{max}} = 330$  nm (Figure 1, dotted trace in inset), consistent with the expected reduction of the imine linkage between the protein and its PLP cofactor. The PLP content of the protein as isolated was estimated by the method of Wada and Snell to be 0.58 equiv (44).

**Spectral Changes Associated with Addition of L-Cysteine to SufS.** The PLP cofactor of the purified enzyme absorbs maximally at 425 nm. Precedent suggests (and the structure discussed below confirms) that the cofactor is in its internal aldimine state (linked as imine to the conserved lysine residue, K231). Addition of sub- or superstoichiometric L-cysteine to this enzyme form leads to a decrease in absorbance at 425 nm and development of a second peak with maximum absorbance at 342 nm (Figure 2A). After addition of superstoichiometric L-cysteine, the new feature persists for minutes, but absorbance in the high-energy regime of the spectrum slowly rises (not shown). The increase has the characteristics of scattering, suggesting that, as has been observed after treatment of other cysteine desulfurases with L-cysteine in the absence of a reductant (2, 4), elemental sulfur accumulates and precipitates. After addition of substoichiometric L-cysteine, the spectrum of the resting enzyme is regenerated on the minutes time scale (Figure 2A,C). Analysis of the dependence of the intensity of the spectral change on the concentration of L-cysteine

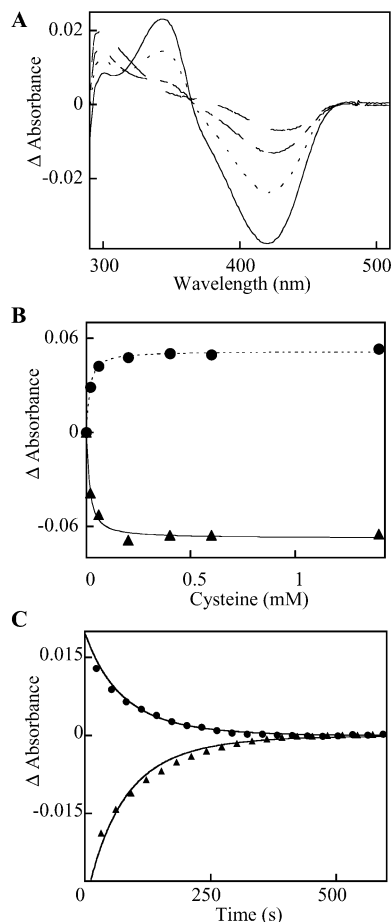


FIGURE 2: Formation and decay of an intermediate upon addition of L-cysteine to SufS. Panel A shows the time-dependent difference spectra after addition of 20  $\mu\text{M}$  L-cysteine to 40  $\mu\text{M}$  SufS. The spectra were acquired 12 (—), 52 (···), 182 (— · —), and 550 s (---) after mixing. Panel B shows the dependence of absorbance at 342 (●) and 425 nm (▲) on concentration of L-cysteine. The solid and dotted lines are fits of the quadratic equation for binding to the data and correspond to a  $K_d$  value of  $11 \pm 6 \mu\text{M}$ . Panel C shows the kinetics of decay of the intermediate monitored at 342 (●) and 425 nm (▲). The solid lines in panel C are simulations of the data according to Scheme 1 with a rate constant for persulfide formation of  $0.02 \pm 0.005 \text{ s}^{-1}$ . In this simulation, the concentration of active SufS was assumed to be 24  $\mu\text{M}$ , corresponding to 40  $\mu\text{M} \times 0.6 \text{ PLP/SufS}$ .

(Figure 2B) allows an apparent dissociation constant of  $11 \pm 6 \mu\text{M}$  to be estimated for the SufS–L-cysteine complex. With this  $K_d$  value, the kinetics of relaxation of the spectrum back toward that of the resting enzyme after addition of substoichiometric L-cysteine (Figure 2C) can be simulated according to a simple two-step mechanism involving rapid-equilibrium binding and a subsequent slow ( $k_1 = 0.020 \pm 0.005 \text{ s}^{-1}$ ) chemical step leading to regeneration of the initial spectrum (Scheme 1).

Addition of either sub- or superstoichiometric L-cysteine to the C372A variant of SufS (SufS-C372A) results in changes in the absorption spectrum identical with those seen for the wild-type enzyme (Figure 3). However, the slow relaxation back to the spectrum of the resting enzyme is not observed with the variant protein (in other words, the adduct is stable in the variant), and the  $K_d$  indicated by titration of this effect is  $600 \pm 100 \mu\text{M}$ . The simplest interpretation of these results is that the C372A substitution diminishes affinity for the substrate by  $\sim 30$ -fold (suggesting the participation

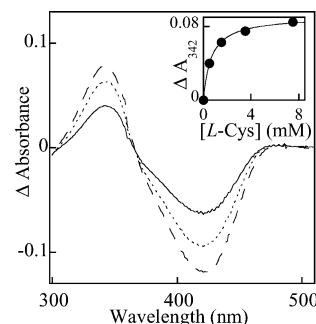
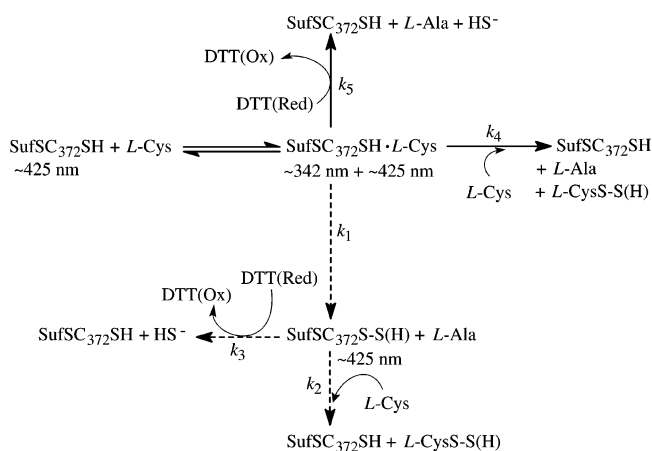


FIGURE 3: Formation of a stable complex between SufS-C372A and L-cysteine. The main panel shows the difference spectra of 50  $\mu\text{M}$  SufS-C372A after addition of 0.5 (—), 1.5 (···), and 7.5 mM (---) L-cysteine. The inset shows the concentration dependence of the spectral change. The solid line in the inset is a fit of the hyperbolic equation for binding to the data and corresponds to a  $K_d$  of  $600 \pm 100 \mu\text{M}$ .

Scheme 1: Kinetic Model for Cysteine Desulfuration by SufS and SufS-C372A<sup>a</sup>



<sup>a</sup> Rate constants are  $k_1 = 0.02 \pm 0.005 \text{ s}^{-1}$ ,  $k_2 = 0.01 \text{ mM}^{-1} \text{ s}^{-1}$ ,  $k_3 = 0.0002 \text{ mM}^{-1} \text{ s}^{-1}$ ,  $k_4 = 0.02 \text{ mM}^{-1} \text{ s}^{-1}$ , and  $k_5 = 0.00015 \text{ mM}^{-1} \text{ s}^{-1}$ . The solid arrows depict steps operant in both SufS and SufS-C372A, and the dotted arrows depict steps operant only in SufS.

of C372 in L-cysteine binding) and that the slow return observed only with the wild-type protein reflects cleavage of the C–S bond of the substrate upon nucleophilic attack by C372 (which cannot occur in the variant).

**Demonstration That Time-Dependent Spectral Change in Wild-Type SufS Corresponds to Cleavage of the C–S Bond of L-Cysteine.** To verify that the slow relaxation of the spectrum of the SufS–L-cysteine complex back to that of the resting enzyme corresponds to cleavage of the C–S bond of the substrate (as opposed to, for example, cleavage of the enzyme persulfide intermediate or release of product alanine), the time dependencies of formation of radiolabeled enzyme and volatilization of sulfur upon incubation of SufS with [<sup>35</sup>S]-L-cysteine were monitored. In the first experiment, the reaction was terminated at various times by heating in SDS, and radiolabeled protein (presumably, the persulfide form) was resolved from unbound and noncovalently bound L-cysteine by denaturing polyacrylamide gel electrophoresis. Quantitative phosphorimage analysis of dried gels (Figure 4A, lower panel) confirmed that the radioactivity associated with the protein does indeed increase on the same time scale as the spectral change. Much less radioactivity (<15%) was associated with the protein in control reactions with the C372A variant (not shown). To define the kinetics of the

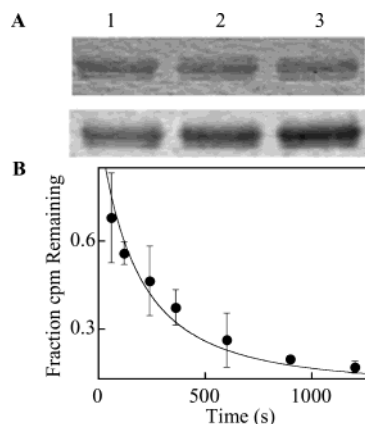


FIGURE 4: Kinetics of SufS persulfide formation upon addition of L-cysteine. Panel A shows the SDS–PAGE analysis of 10  $\mu$ M SufS denatured 10 s (lane 1), 45 s (lane 2), and 2 min (lane 3) after treatment with 5  $\mu$ M [ $^{35}$ S]-L-cysteine. The top panel shows the results of Coomassie staining, and the bottom panel shows the results of phosphorimage analysis. Panel B shows the kinetics of radioactivity remaining following reductive quenching and acidification of the reaction of SufS (10  $\mu$ M) and [ $^{35}$ S]-L-cysteine (5  $\mu$ M). The solid line in panel B is a simulation according to Scheme 1.

process more accurately and avoid the potential complication of adventitious disulfide formation between the radiolabeled substrate and the protein occurring as a result of the absence of reductant in this first experiment, the complementary approach of terminating the reaction by heating in a denaturing solution (SDS or guanidine) containing a high concentration (100 mM) of the reductant, DTT, was taken. In this experiment, the radioactivity not volatilized by the reducing, denaturing quench (corresponding to the remaining substrate) was quantified. As shown in Figure 4B, the kinetics of volatilization can be simulated quite well according to the same kinetic scheme (Scheme 1) used to reproduce the spectral kinetic data. These results confirm that the slow spectral changes are indeed a reflection of formation of the SufS persulfide species upon nucleophilic attack by C372. This conclusion suggests that the SufS–L-cysteine complex represents an equilibrium mixture of L-cysteine aldimine and ketimine complexes. On the basis of published mechanistic proposals (51), the latter should be the species that reacts by attack of the nucleophilic C372 on the substrate sulfur.

**Steady-State Kinetic Analysis of SufS and SufS-C372A.** The dependencies of the turnover rates of the wild-type protein (Figure 5A) and C372A variant (Figure 5B) on the concentration of L-cysteine in the presence of 50 mM dithiothreitol are unusual in that saturation is not observed. Their near-linearity at concentrations of L-cysteine much higher than  $K_d$  suggests the participation of unbound substrate in some fashion. The significant activity of the variant protein is even more surprising, because the corresponding substitution has been reported to completely inactivate other cysteine desulfurases (28, 41, 51–53). Close inspection of the low L-cysteine concentration regime of the two plots reveals that the activity of the wild-type protein initially increases more steeply with increasing L-cysteine concentration than does the activity of the C372A variant. Thus, this initial phase must reflect the contribution from nucleophilic attack by C372 to form a cysteinyl persulfide intermediate and subsequent reductive cleavage of the persulfide. The unsaturating, linear phase in the plots for both the wild-type and

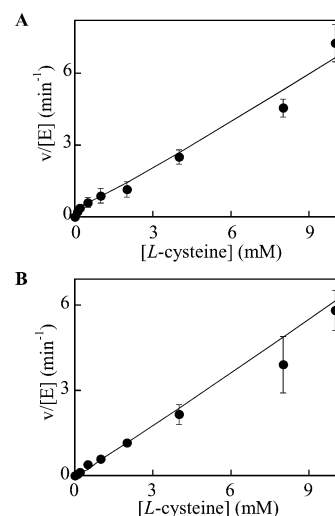


FIGURE 5: Dependence of the cysteine desulfurase activity of (A) SufS and (B) SufS-C372A on L-cysteine concentration. The solid lines are simulations according to Scheme 1.

C372A proteins must reflect desulfuration by a different mechanism. Given the deduction that unbound L-cysteine is involved and the fact that C372 is not required, this component of the overall steady-state turnover rate most likely arises from direct attack of the sulfhydryl group of a second, unbound molecule of L-cysteine on the sulfur of the L-cysteine–ketimine adduct to form alanine and (small-molecule) L-cysteine persulfide (Scheme 1). The dependence of the steady-state rate of the wild-type protein on L-cysteine concentration can be simulated (solid line in Figure 5A) as the resultant of these two pathways (Scheme 1) with the rate constant for the nucleophilic attack by C372 assumed to be that determined in the single-turnover experiments ( $0.020 \pm 0.005 \text{ s}^{-1}$ ). The plot for the C372A variant can also be reproduced (solid line in Figure 5B) by assuming the same rate constant for the attack by the second molecule of L-cysteine and the higher measured  $K_d$  for the variant of  $600 \pm 100 \mu\text{M}$ . Of course, the pathway involving the C372 persulfide intermediate is assumed not to be operant in the variant protein.

The first conclusion that may be drawn from the kinetic data is that cysteine desulfuration by SufS is very inefficient. Similar inefficiency has been documented for SufS proteins from other organisms (17, 28, 30, 52). It would seem that activation by accessory factors, as has been shown to occur when the SufS proteins from *E. coli* and *Erwinia chrysanthemi* bind to SufE (28–30), would be required to allow SufS to serve as the primary provider of sulfur for synthesis of FeS clusters and other cofactors in *Synechocystis* sp. PCC 6803 (as is implied by the genetic results) (33).<sup>2</sup> Interestingly, the *suf* operon of this bacterium lacks a homologue of the *sufE* gene (31, 32). However, a hypothetical protein with 35% identity to the SufE proteins from both *E. coli* and *Erwinia chrysanthemi* is encoded elsewhere in the genome by *slr1419*. Experiments are in progress to determine whether the Slr1419 protein functions as a SufE homologue by binding to and activating SufS.

A second implication of the kinetic analysis is that cleavage of the C–S bond of the substrate upon attack by C372 is extremely sluggish in SufS ( $0.02 \text{ s}^{-1}$ ). By contrast, our analysis of the kinetics of Slr0387, a sequence group I (Nif/IscS-like) desulfurase from the same organism, indicates



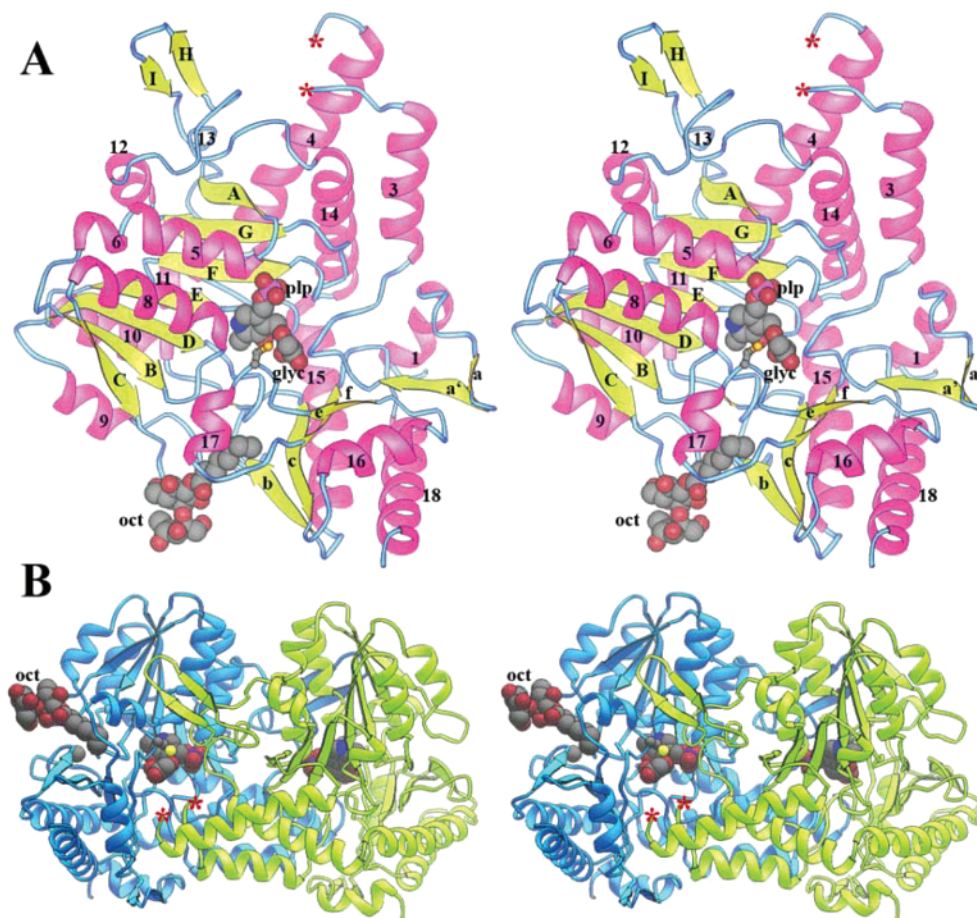


FIGURE 6: Overall fold of SufS. Panel A shows a stereoview of the crystal structure of SufS monomer with secondary structural elements labeled as in ref 58. Strands in the large domain are capital letters, strands in the small domain are lowercase letters, and helices are numbered. PLP, glycerol (labeled "glyc"), active site cysteine C372, and *n*-octanoyl sucrose (labeled "OCT") are depicted in space-filling format. Several secondary structural elements in SufS differ from those in *E. coli* SufS: helices 2, 7, and 13 from *E. coli* SufS are absent in SufS, and strand d of the *E. coli* enzyme is missing in SufS, replaced spatially by strand a'. The chain break between helices 3 and 4 is marked with two red asterisks. Panel B shows a stereoview of the SufS dimer with one chain colored blue and the other colored yellow. PLP, glycerol, active site cysteine (C372), and *n*-octanoyl sucrose (labeled OCT) are depicted in space-filling format, and the chain break is denoted with two red asterisks.

that the nucleophilic attack step has a rate constant of  $>20 \text{ s}^{-1}$  and is not rate-limiting (43). Thus, for SufS to be activated by binding to accessory factors (e.g., Slr1419), it would seem that cleavage of the C–S bond of the substrate would have to be accelerated. By contrast, the previous studies demonstrating activation of SufS proteins by binding to SufE have implied that activation occurs by acceleration of the breakdown of the SufS persulfide as a consequence of the ability of SufE to accept sulfur from this intermediate to form a SufE cysteinyl persulfide species (29). Our data suggest that, rather than merely positioning a cysteine residue for this sulfur transfer, binding of accessory proteins to activate SufS would have to perturb the structure or dynamics of the protein in the region of C372 to accelerate its attack on the substrate sulfur. Alternatively, binding of an accessory protein could position one of the cysteine residues of the accessory protein for *intermolecular* attack (analogous to attack by a second molecule of L-cysteine) on the substrate sulfur. These possibilities are being tested.

**Crystal Structure of SufS.** As expected, the 1.8 Å structure of SufS (Figure 6A) reveals its close structural similarity to *E. coli* SufS (47) (RMSD 1.1 Å over 401 Cα atoms, 49% sequence identity, all as calculated by Dali (54)), *T. maritima* IscS (55) (RMSD 2.1 Å over 353 Cα atoms, 27% sequence

identity), and other PLP-dependent proteins, such as C-DES (56) (RMSD 2.3 Å over 361 Cα atoms and 26% identity), and phosphoserine aminotransferase (57) (RMSD 3.3 Å over 331 Cα atoms, 12% identity). The dimeric SufS is a member of the α-family of PLP-dependent enzymes and consists of two domains, a large domain that binds PLP and a smaller domain that harbors the active site cysteine (Figure 6B). The active site is located at the dimerization interface and between the large and small domains, with residues from both monomers contributing.

Pyridoxal-5'-phosphate is observed covalently linked to K231 of each monomer, and a molecule of glycerol can be seen in electron density maps in each active site, bound where substrate is expected to bind on the basis of previous structures of *E. coli* SufS and other related PLP-dependent enzymes (Figure 7A). Because the crystals had a yellow color before and after data collection, it was assumed that the PLP cofactor was in its oxidized form. Interestingly, the bond between C4a of the cofactor and Nζ of K231 is not coplanar with the pyridine ring of the cofactor (Figure 7B). Coplanarity would be expected from the results of small molecule crystallography and has been seen in enzymes such as phosphoserine aminotransferase (PDB ID 1bjn). However, the crystal structures of many other PLP-containing enzymes

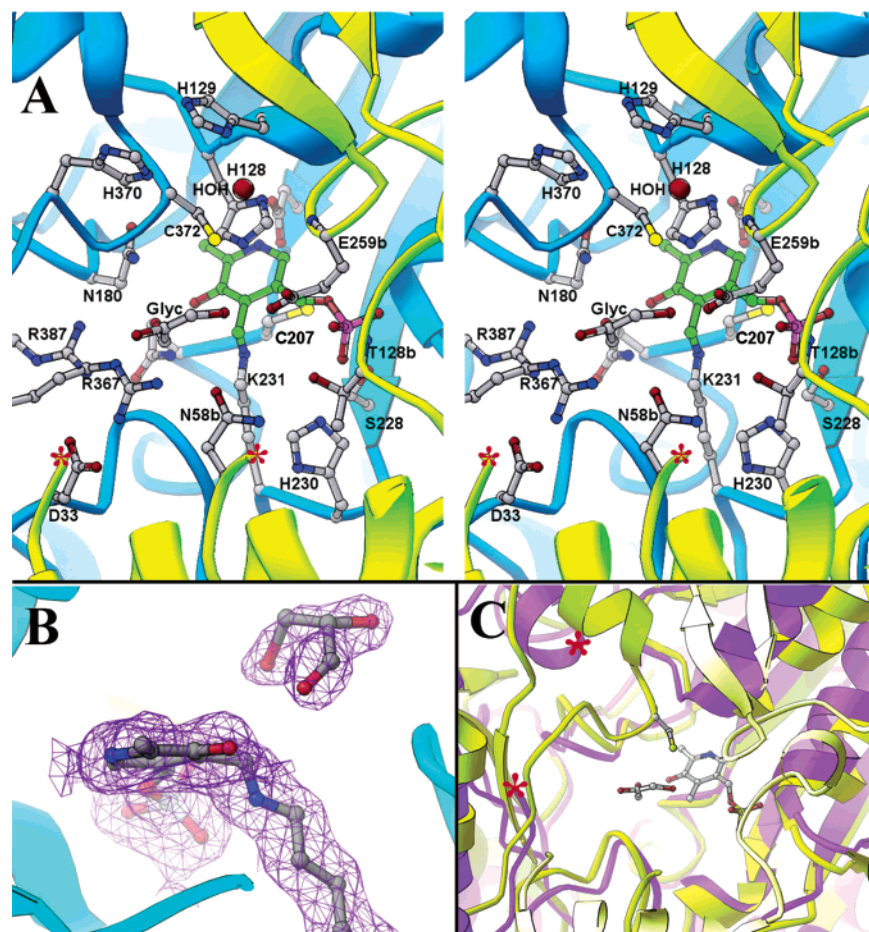


FIGURE 7: Views of the SufS active site. Panel A shows a stereoview of the SufS active site. The carbons of the PLP are colored green, and side chains near the active site are labeled by one-letter abbreviation and number (carbons colored gray, oxygen red, nitrogen blue, sulfur yellow, and phosphorus magenta). The two monomers are colored as described in Figure 6B, and side chains from the yellow chain are labeled with one-letter abbreviation, number, and a lowercase b. Glycerol bound at the active site is labeled "Glyc". Two red asterisks indicate the chain break between helices 3 and 4. Panel B shows a  $2F_o - F_c$  composite omit electron density map contoured at  $1\sigma$  shown around the covalently bound PLP cofactor and glycerol in the active site. Atoms are colored as described in panel A. Panel C shows the superposition of SufS (yellow) and IscS from *T. maritima* (1ECX, purple). C372, PLP, and glycerol are depicted in ball-and-stick and are colored as described in panel A. In this case, the red asterisks denote where traceable density ends as a result of the disordered IscS active site loop (see text).

exhibit this nonplanarity (see, for example, PDB IDs 1qop (58) and 1b54 (59)). The yellow color did not diffuse out of crystals upon soaking in a drop of reservoir solution but did disappear upon treatment of the crystals with sodium borohydride. Electron density calculated from data collected on reduced protein crystals appeared similar to that of the "oxidized" crystals in the region of the PLP linkage, though the quality of the electron density was considerably poorer. No adventitiously bound PLP, which could have explained the crystal color, was observed in the electron density. These observations confirm that PLP is indeed linked as an imine to K231 and suggest that the imine linkage was perhaps photoreduced during data collection.

Differences with respect to the previously determined structure of *E. coli* SufS are limited primarily to short insertions and deletions and minor differences in assigned secondary structure. Notable differences in the active site (Figure 7A) include several conservative substitutions (such as A207C, which packs against the PLP cofactor) and increased disorder of the loop connecting helices 3 and 4. The disorder implicates this loop in facilitating substrate diffusion and perhaps in interactions between SufS and other proteins. A notable similarity between this structure and that

of *E. coli* SufS is that the loop containing C372 is structurally well-defined. By contrast, the longer loop in the sequence group I (Nif/IscS-like) CD from *T. maritima* was determined to be structurally disordered (Figure 7C). The shortness and decreased flexibility of this loop in the SufS proteins is likely relevant to their well-documented catalytic inefficiency and to our conclusion that the sluggishness of attack by the nucleophilic cysteine residue is the primary cause of this inefficiency (17, 28, 30, 52). In the absence of bound substrate, it is not possible to predict what structural changes might be necessary to accelerate this step, but the general prediction can be advanced that structures of SufS–SufE complexes should reveal significant alterations of the SufS structure in the region of C372.

One final interesting observation is the presence of a bound detergent (*n*-octanoyl sucrose) molecule, which was included in the crystallization conditions as part of a Hampton additive screen to improve crystal quality. The sucrose moiety is visible at a crystal lattice contact, where its hydrocarbon chain can be seen inserted between the two domains of one polypeptide chain, the last carbon positioned 11 Å from the active site cysteine (Figure 6). Because it is observed in only one monomer of the dimer, the second chain was used to



investigate differences caused by detergent binding. Structural rearrangements in the area surrounding the detergent are limited to movement of F380 (4.5 Å) and slight (approximately 0.5 Å) adjustment of the backbone and side chains immediately adjacent to the detergent. No structural rearrangements in the active site are observed. Although the detergent itself is not physiologically relevant, it is possible that it occupies the binding site of activating accessory factors.

## SUPPORTING INFORMATION AVAILABLE

SDS–PAGE gel showing overexpression of the SufS protein and its N-terminally modified forms; explanation of problems encountered in attempts to overexpress native SufS in standard host strains. This material is available free of charge via the Internet at <http://pubs.acs.org>.

## REFERENCES

- Jacobson, M. R., Cash, V. L., Weiss, M. C., Laird, N. F., Newton, W. E., and Dean, D. R. (1989) Biochemical and genetic analysis of the *nifUSVWZM* cluster from *Azotobacter vinelandii*, *Mol. Gen. Genet.* 219, 49–57.
- Zheng, L., White, R. H., Cash, V. L., Jack, R. F., and Dean, D. R. (1993) Cysteine desulfurase activity indicates a role for NIFS in metallocluster biosynthesis, *Proc. Natl. Acad. Sci. U.S.A.* 90, 2754–2758.
- Zheng, L., and Dean, D. R. (1994) Catalytic formation of a nitrogenase iron–sulfur cluster, *J. Biol. Chem.* 269, 18723–18726.
- Flint, D. H. (1996) *Escherichia coli* contains a protein that is homologous in function and N-terminal sequence to the protein encoded by the *nifS* gene of *Azotobacter vinelandii* and that can participate in the synthesis of the Fe–S cluster of dihydroxy-acid dehydratase, *J. Biol. Chem.* 271, 16068–16074.
- Zheng, L., Cash, V. L., Flint, D. H., and Dean, D. R. (1998) Assembly of iron–sulfur clusters. Identification of an *iscSUA-hscBA-fdx* gene cluster from *Azotobacter vinelandii*, *J. Biol. Chem.* 273, 13264–13272.
- Li, J., Kogan, M., Knight, S. A., Pain, D., and Dancis, A. (1999) Yeast mitochondrial protein, Nfs1p, coordinately regulates iron–sulfur cluster proteins, cellular iron uptake, and iron distribution, *J. Biol. Chem.* 274, 33025–33034.
- Agar, J. N., Krebs, C., Frazzon, J., Huynh, B. H., Dean, D. R., and Johnson, M. K. (2000) IscU as a scaffold for iron–sulfur cluster biosynthesis: sequential assembly of [2Fe–2S] and [4Fe–4S] clusters in IscU, *Biochemistry* 39, 7856–7862.
- Krebs, C., Agar, J. N., Smith, A. D., Frazzon, J., Dean, D. R., Huynh, B. H., and Johnson, M. K. (2001) IscA, an alternate scaffold for Fe–S cluster biosynthesis, *Biochemistry* 40, 14069–14080.
- Kispal, G., Csere, P., Prohl, C., and Lill, R. (1999) The mitochondrial proteins Atm1p and Nfs1p are essential for biogenesis of cytosolic Fe/S proteins, *EMBO J.* 18, 3981–3989.
- Kurihara, T., Mihara, H., Kato, S., Yoshimura, T., and Esaki, N. (2003) Assembly of iron–sulfur clusters mediated by cysteine desulfurases, IscS, CsdB and CSD, from *Escherichia coli*, *Biochim. Biophys. Acta* 1647, 303–309.
- Begley, T. P., Ealick, S. E., McLafferty, F. W., Van Loon, A. P., Taylor, S., Campobasso, N., Chiu, H. J., Kinsland, C., Reddick, J. J., and Xi, J. (1999) Thiamin biosynthesis in prokaryotes, *Arch. Microbiol.* 171, 293–300.
- Lauhon, C. T., and Kambampati, R. (2000) The *iscS* gene in *Escherichia coli* is required for the biosynthesis of 4-thiouridine, thiamin, and NAD, *J. Biol. Chem.* 275, 20096–20103.
- Leimkuhler, S., and Rajagopalan, K. V. (2001) A sulfurtransferase is required in the transfer of cysteine sulfur in the *in vitro* synthesis of molybdopterin from precursor Z in *Escherichia coli*, *J. Biol. Chem.* 276, 22024–22031.
- Kambampati, R., and Lauhon, C. T. (1999) IscS is a sulfurtransferase for the *in vitro* biosynthesis of 4-thiouridine in *Escherichia coli* tRNA, *Biochemistry* 38, 16561–16568.
- Mueller, E. G., Palenchar, P. M., and Buck, C. J. (2001) The role of the cysteine residues of ThiI in the generation of 4-thiouridine in tRNA, *J. Biol. Chem.* 276, 33588–33595.
- Lauhon, C. T. (2002) Requirement for IscS in biosynthesis of all thionucleosides in *Escherichia coli*, *J. Bacteriol.* 184, 6820–6829.
- Mihara, H., Kurihara, T., Yoshimura, T., Soda, K., and Esaki, N. (1997) Cysteine sulfinic desulfinase, a NIFS-like protein of *Escherichia coli* with selenocysteine lyase and cysteine desulfurase activities. Gene cloning, purification, and characterization of a novel pyridoxal enzyme, *J. Biol. Chem.* 272, 22417–22424.
- Jacobson, M. R., Brigle, K. E., Bennett, L. T., Setterquist, R. A., Wilson, M. S., Cash, V. L., Beynon, J., Newton, W. E., and Dean, D. R. (1989) Physical and genetic map of the major *nif* gene cluster from *Azotobacter vinelandii*, *J. Bacteriol.* 171, 1017–1027.
- Patzer, S. I., and Hantke, K. (1999) SufS is a NifS-like protein, and SufD is necessary for stability of the [2Fe–2S] FhuF protein in *Escherichia coli*, *J. Bacteriol.* 181, 3307–3309.
- Olson, J. W., Agar, J. N., Johnson, M. K., and Maier, R. J. (2000) Characterization of the NifU and NifS Fe–S cluster formation proteins essential for viability in *Helicobacter pylori*, *Biochemistry* 39, 16213–16219.
- Schwartz, C. J., Djaman, O., Imlay, J. A., and Kiley, P. J. (2000) The cysteine desulfurase, IscS, has a major role in *in vivo* Fe–S cluster formation in *Escherichia coli*, *Proc. Natl. Acad. Sci. U.S.A.* 97, 9009–9014.
- Ellis, K. E., Clough, B., Saldanha, J. W., and Wilson, R. J. (2001) NifS and SufS in malaria, *Mol. Microbiol.* 41, 973–981.
- Nachin, L., El Hassouni, M., Loiseau, L., Expert, D., and Barras, F. (2001) SoxR-dependent response to oxidative stress and virulence of *Erwinia chrysanthemi*: the key role of SufC, an orphan ABC ATPase, *Mol. Microbiol.* 39, 960–972.
- Ollagnier-de Choudens, S., Nachin, L., Sanakis, Y., Loiseau, L., Barras, F., and Fontecave, M. (2003) SufA from *Erwinia chrysanthemi*. Characterization of a scaffold protein required for iron–sulfur cluster assembly, *J. Biol. Chem.* 278, 17993–18001.
- Zheng, M., Wang, X., Templeton, L. J., Smulski, D. R., LaRossa, R. A., and Storz, G. (2001) DNA microarray-mediated transcriptional profiling of the *Escherichia coli* response to hydrogen peroxide, *J. Bacteriol.* 183, 4562–4570.
- Wang, T., Shen, G., Balasubramanian, R., McIntosh, L., Bryant, D. A., and Golbeck, J. H. (2004) The *sufR* gene (*slr0088* in *Synechocystis* sp. strain PCC 6803) functions as a repressor of the *sufBCDS* operon in iron–sulfur cluster biogenesis in cyanobacteria, *J. Bacteriol.* 186, 956–967.
- Takahashi, Y., and Tokumoto, U. (2002) A third bacterial system for the assembly of iron–sulfur clusters with homologues in archaea and plastids, *J. Biol. Chem.* 277, 28380–28383.
- Loiseau, L., Ollagnier-de-Choudens, S., Nachin, L., Fontecave, M., and Barras, F. (2003) Biogenesis of Fe–S clusters by the bacterial Suf system: SufS and SufE form a new type of cysteine desulfurase, *J. Biol. Chem.* 278, 38352–38359.
- Ollagnier-de-Choudens, S., Lascoux, D., Loiseau, L., Barras, F., Forest, E., and Fontecave, M. (2003) Mechanistic studies of the SufS–SufE cysteine desulfurase: evidence for sulfur transfer from SufS to SufE, *FEBS Lett.* 555, 263–267.
- Outten, F. W., Wood, M. J., Munoz, F. M., and Storz, G. (2003) The SufE protein and the SufBCD complex enhance SufS cysteine desulfurase activity as part of a sulfur transfer pathway for Fe–S cluster assembly in *Escherichia coli*, *J. Biol. Chem.* 278, 45713–45719.
- Ikeuchi, M. (1996) Complete genome sequence of a cyanobacterium *Synechocystis* sp. PCC 6803, the oxygenic photosynthetic prokaryote, *Tanpakushitsu Kakusan Koso* 41, 2579–2583.
- Kaneko, T., Sato, S., Kotani, H., Tanaka, A., Asamizu, E., Nakamura, Y., Miyajima, N., Hirasawa, M., Sugura, M., Sasamoto, S., Kimura, T., Hosouchi, T., Matsuno, A., Muraki, A., Nakazaki, N., Naruo, K., Okumura, S., Shimpo, S., Takeuchi, C., Wada, T., Watanabe, A., Yamada, M., Yasuda, M., and Tabata, S. (1996) Sequence analysis of the genome of the unicellular cyanobacterium *Synechocystis* sp. strain PCC6803. II. Sequence determination of the entire genome and assignment of potential protein-coding regions, *DNA Res.* 3, 109–136.
- Seidler, A., Jaschke, K., and Wollenberg, M. (2001) Incorporation of iron–sulfur clusters in membrane-bound proteins, *Biochem. Soc. Trans.* 29, 418–421.
- Kobayashi, K., Ehrlich, S. D., Albertini, A., Amati, G., Andersen, K. K., Arnaud, M., Asai, K., Ashikaga, S., Aymerich, S., Bessieres, P., Boland, F., Brignell, S. C., Bron, S., Bunai, K., Chapuis, J., Christiansen, L. C., Danchin, A., Debarbouille, M., Dervyn, E., Deuerling, E., Devine, K., Devine, S. K., Dreesen, O., Errington, J., Fillinger, S., Foster, S. J., Fujita, Y., Galizzi, A., Gardan, R., Eschevins, C., Fukushima, T., Haga, K., Harwood, C. R., Hecker,

- M., Hosoya, D., Hullo, M. F., Kakeshita, H., Karamata, D., Kasahara, Y., Kawamura, F., Koga, K., Koski, P., Kuwana, R., Imamura, D., Ishimaru, M., Ishikawa, S., Ishio, I., Le Coq, D., Masson, A., Mauel, C., Meima, R., Mellado, R. P., Moir, A., Moriya, S., Nagakawa, E., Nanamiya, H., Nakai, S., Nygaard, P., Ogura, M., Ohanan, T., O'Reilly, M., O'Rourke, M., Pragai, Z., Pooley, H. M., Rapoport, G., Rawlins, J. P., Rivas, L. A., Rivolta, C., Sadaie, A., Sadaie, Y., Sarvas, M., Sato, T., Saxild, H. H., Scanlan, E., Schumann, W., Seegers, J. F., Sekiguchi, J., Sekowska, A., Seror, S. J., Simon, M., Stragier, P., Studer, R., Takamatsu, H., Tanaka, T., Takeuchi, M., Thomaidis, H. B., Vagner, V., van Dijk, J. M., Watabe, K., Wipat, A., Yamamoto, H., Yamamoto, M., Yamamoto, Y., Yamane, K., Yata, K., Yoshida, K., Yoshikawa, H., Zuber, U., and Ogasawara, N. (2003) Essential *Bacillus subtilis* genes, *Proc. Natl. Acad. Sci. U.S.A.* 100, 4678–4683.
35. Takahashi, Y., Mitsui, A., Fujita, Y., and Matsubara, H. (1991) Roles of ATP and NADPH in formation of the Fe–S cluster of spinach Ferredoxin, *Plant Physiol.* 39, 104–110.
36. Pilon-Smits, E. A., Garifullina, G. F., Abdel-Ghany, S., Kato, S., Mihara, H., Hale, K. L., Burkhead, J. L., Esaki, N., Kurihara, T., and Pilon, M. (2002) Characterization of a NifS-like chloroplast protein from *Arabidopsis*. Implications for its role in sulfur and selenium metabolism, *Plant Physiol.* 130, 1309–1318.
37. Léon, S., Touraine, B., Briat, J.-F., and Lobréaux, S. (2002) The *AtNFS2* gene from *Arabidopsis thaliana* encodes a NifS-like plastidial cysteine desulfurase, *Biochem. J.* 366, 557–564.
38. Wittpoth, C., Kroth-Pancic, P. G., and Strotmann, H. (1996) Overexpression and localization of an unknown plastid encoded protein in the diatom *Odontella sinensis* with similarities to a subunit of ABC-transporters, *Plant Sci.* 114, 171–179.
39. Moller, S. G., Kunkel, T., and Chua, N. H. (2001) A plastidic ABC protein involved in intercompartmental communication of light signaling, *Genes Dev.* 15, 90–103.
40. Kushnir, S., Babyichuk, E., Storozhenko, S., Davey, M. W., Papenbrock, J., De Rycke, R., Engler, G., Stephan, U. W., Lange, H., Kispal, G., Lill, R., and Van Montagu, M. (2001) A mutation in the mitochondrial ABC transporter *Sta1* leads to dwarfism and chlorosis in the *Arabidopsis* mutant *starik*, *Plant Cell* 13, 89–100.
41. Jaschkowitz, K., and Seidler, A. (2000) Role of a NifS-like protein from the cyanobacterium *Synechocystis* PCC 6803 in the maturation of FeS proteins, *Biochemistry* 39, 3416–3423.
42. Kato, S., Mihara, H., Kurihara, T., Yoshimura, T., and Esaki, N. (2000) Gene cloning, purification, and characterization of two cyanobacterial NifS homologues driving iron–sulfur cluster formation, *Biosci. Biotechnol. Biochem.* 64, 2412–2419.
43. Behshad, E., Parkin, S. A., Bollinger, J. M., Jr. (2004) Mechanism of Cysteine Desulfurase Slr0387 from *Synechocystis* sp. PCC 6803: Kinetic Analysis of Cleavage of the Persulfide Intermediate by Chemical Reductants, *Biochemistry* 43, 12220–12226.
44. Wada, H., and Snell, E. E. (1961) The enzymatic oxidation of pyridoxine and pyridoxamine phosphates, *J. Biol. Chem.* 236, 2089–2095.
45. Otwinowski, Z., and Minor, W. (1997) Processing of X-ray Diffraction Data Collected in Oscillation Mode, in *Macromolecular Crystallography. Part A* (Carter, C. W. Jr. and Sweet, R. M., Eds.) Methods in Enzymology Vol. 276, pp 307–326, Academic Press, San Diego, CA.
46. Navaza, J. (1994) AMoRe: An automated package for molecular replacement., *Acta Crystallogr. A* 50, 157–163.
47. Lima, C. D. (2002) Analysis of the *E. coli* NifS CsdB protein at 2.0 Å reveals the structural basis for perselenide and persulfide intermediate formation, *J. Mol. Biol.* 315, 1199–1208.
48. Brunger, A. T., Adams, P. D., Clore, G. M., Gros, P., Grosse-Kunstleve, R. W., Jiang, J.-S., Kuszewski, J., Nilges, N., Pannu, N. S., Read, R. J., Rice, L. M., Simonson, T., and Warren, G. L. (1998) Crystallography & NMR system (CNS): A new software system for macromolecular structure determination, *Acta Crystallogr. D* 54, 905–921.
49. McRee, D. E. (1993) *Practical Protein Crystallography*, Academic Press, San Diego, CA.
50. McRee, D. E. (1999) XtalView/Xfit – A Versatile Program for Manipulating Atomic Coordinates and Electron Density, *J. Struct. Biol.* 125, 156–165.
51. Zheng, L., White, R. H., Cash, V. L., and Dean, D. R. (1994) Mechanism for the desulfurization of L-cysteine catalyzed by the *nifS* gene product, *Biochemistry* 33, 4714–4720.
52. Mihara, H., Kurihara, T., Yoshimura, T., and Esaki, N. (2000) Kinetic and mutational studies of three NifS homologues from *Escherichia coli*: mechanistic difference between L-cysteine desulfurase and L-selenocysteine lyase reactions, *J. Biochem. (Tokyo)* 127, 559–567.
53. Urbina, H. D., Silberg, J. J., Hoff, K. G., and Vickery, L. E. (2001) Transfer of sulfur from IscS to IscU during Fe/S cluster assembly, *J. Biol. Chem.* 276, 44521–44526.
54. Holm, L. S. C. (1993) Protein structure comparison by alignment of distance matrices, *J. Mol. Biol.* 233, 123–138.
55. Kaiser, J. T., Clausen, T., Bourenkow, G. P., Bartunik, H. D., Steinbacher, S., and Huber, R. (2000) Crystal structure of a NifS-like protein from *Thermotoga maritima*: implications for iron sulphur cluster assembly, *J. Mol. Biol.* 297, 451–464.
56. Clausen, T., Kaiser, J. T., Steegborn, C., Huber, R., and Kessler, D. (2000) Crystal structure of the cystine C–S lyase from *Synechocystis*: stabilization of cysteine persulfide for FeS cluster biosynthesis, *Proc. Natl. Acad. Sci. U.S.A.* 97, 3856–3861.
57. Hester, G., Stark, W., Moser, M., Kallen, J., Markovic-Housley, Z., and Jansonius, J. N. (1999) Crystal structure of phosphoserine aminotransferase from *Escherichia coli* at 2.3 Å resolution: comparison of the unligated enzyme and a complex with  $\alpha$ -methyl-L-glutamate, *J. Mol. Biol.* 286, 829–850.
58. Weyand, M., and Schlichting, I. (1999) Crystal structure of wild-type tryptophan synthase complexed with the natural substrate indole-3-glycerol phosphate, *Biochemistry* 38, 16469–16480.
59. Eswaramoorthy, S., Gerchman, S., Graziano, V., Kycia, H., Studier, F. W., and Swaminathan, S. (2003) Structure of a yeast hypothetical protein selected by a structural genomics approach, *Acta Crystallogr. Sect. D: Biol. Crystallogr.* 59, 127–135.
60. Mihara, H., Kato, S., Lacourciere, G. M., Stadtman, T. C., Kennedy, R. A., Kurihara, T., Tokumoto, U., Takahashi, Y., and Esaki, N. (2002) The *iscS* gene is essential for the biosynthesis of 2-selenouridine in tRNA and the selenocysteine-containing formate dehydrogenase H, *Proc. Natl. Acad. Sci. U.S.A.* 99, 6679–6683.

BI0491447